THE JOURNAL OF BIOLOGICAL CHEMISTRY
Vol. 278, No. 26, Issue of June 27, pp. 23738–23746, 2003

Printed in U.S.A.

Caveolin Interacts with the Angiotensin II Type 1 Receptor during Exocytic Transport but Not at the Plasma Membrane*

Received for publication, December 18, 2002, and in revised form, April 8, 2003
Published, JBC Papers in Press, April 13, 2003, DOI 10.1074/jbc.M212892200

Bruce D. Wyse‡§, Ian A. Prior‡§, Hongwei Qian¶, Isabel C. Morrow‡‖, Susan Nixon‡‖, Cornelia Muncke‡§, Teymuras V. Kurzchalia, Walter G. Thomas¶, Robert G. Parton‡‖, and John F. Hancock‡§‡‡**

*From the ‡Institute for Molecular Bioscience, the §Department of Molecular and Cellular Pathology, and the ‖Centre for Microscopy and Microanalysis and School of Biomedical Sciences, University of Queensland, Brisbane, 4072 Queensland, Australia, the ¶Baker Heart Research Institute, Melbourne, 3004 Victoria, Australia, and the **Max Planck Institute for Molecular Cell Biology and Genetics, Dresden D-01307, Germany*

The mechanisms involved in angiotensin II type 1 receptor (AT_1-R) trafficking and membrane localization are largely unknown. In this study, we examined the role of caveolin in these processes. Electron microscopy of plasma membrane sheets shows that the AT_1-R is not concentrated in caveolae but is clustered in cholesterol-independent microdomains; upon activation, it partially redistributes to lipid rafts. Despite the lack of AT_1-R in caveolae, AT_1-R·caveolin complexes are readily detectable in cells co-expressing both proteins. This interaction requires an intact caveolin scaffolding domain because mutant caveolins that lack a functional caveolin scaffolding domain do not interact with AT_1-R. Expression of an N-terminally truncated caveolin-3, CavDGV, that localizes to lipid bodies, or a point mutant, Cav3-P104L, that accumulates in the Golgi mislocalizes AT_1-R to lipid bodies and Golgi, respectively. Mislocalization results in aberrant maturation and surface expression of AT_1-R, effects that are not reversed by supplementing cells with cholesterol. Similarly mutation of aromatic residues in the caveolin-binding site abrogates AT_1-R cell surface expression. In cells lacking caveolin-1 or caveolin-3, AT_1-R does not traffic to the cell surface unless caveolin is ectopically expressed. This observation is recapitulated in caveolin-1 null mice that have a 55% reduction in renal AT_1-R levels compared with controls. Taken together our results indicate that a direct interaction with caveolin is required to traffic the AT_1-R through the exocytic pathway, but this does not result in AT_1-R sequestration in caveolae. Caveolin therefore acts as a molecular chaperone rather than a plasma membrane scaffold for AT_1-R.

Lipid-based sorting mechanisms play an important role in the organization of the plasma membrane into microdomains (1–3). The biophysical properties of sphingolipids and cholesterol drive the spontaneous formation of lateral assemblies of liquid-ordered lipid rafts in a sea of liquid-disordered phospholipids. The biological importance of lipid rafts follows from the lateral segregation that they impose on membrane proteins. The differential distribution of plasma membrane proteins across raft and nonraft membranes in turn results in the concentration of specific groups of signaling proteins and lipids within discrete areas of the cell membrane (3–6). This increases the efficiency and specificity of signaling events by allowing more efficient interactions between proteins and by preventing cross-talk between different pathways.

Caveolae are an abundant surface feature of many mammalian cells and represent a specific subtype of lipid raft. Functionally, caveolae have been implicated in endocytosis (7), potocytosis (8), transcytosis (9), apical transport (10), and cholesterol balance (11). Caveolae are identified by their characteristic morphology (flask-shaped, 55–65-nm diameter pits) and the presence of integral membrane proteins, termed caveolins, of which three mammalian isoforms have been characterized (caveolin-1, -2, and -3) (12–14). Caveolins show the characteristic biochemical features of raft-associated proteins, being associated with low density detergent-insoluble complexes that are sensitive to cholesterol depletion (15, 16). Caveolins are crucial structural components of caveolae. Expression of caveolin-1 in cells lacking caveolae causes *de novo* formation of caveolae, whereas ablation of caveolin expression causes a loss of caveolae in cultured cells and *in vivo* (17, 18). The ability of caveolins to bind cholesterol and to form high molecular weight oligomeric complexes is presumably important in caveolae formation. Caveolin-1 and caveolin-2 form hetero-oligomeric complexes and are most prevalent in endothelial cells, smooth muscle cells, skeletal myoblasts, fibroblasts, and adipocytes (19), whereas caveolin-3 (Cav3)[1] is exclusively present in muscle cells including cardiac myocytes and cells of the arterial vasculature (20).

As well as this structural role, caveolins have also been directly implicated in interactions with signaling proteins. A juxtamembrane region of caveolin, the caveolin scaffolding domain (CSD) binds *in vitro* to a consensus sequence of $\Phi X\Phi XXXX\Phi XX\Phi$ (where Φ is an aromatic amino acid and X is any amino acid) that is found in a large number of signaling proteins including G-proteins, conserved kinase domain IX, and elsewhere in many nonkinases (21–23). Caveolin has therefore been postulated to act as a protein scaffold for sig-

* This work is supported by grants from the National Health and Medical Research Council of Australia (to J. F. H. and R. G. P.) and Queensland Cancer Fund (to J. F. H.). The Institute for Molecular Bioscience is a Special Research Center of the Australian Research Council. The costs of publication of this article were defrayed in part by the payment of page charges. This article must therefore be hereby marked "*advertisement*" in accordance with 18 U.S.C. Section 1734 solely to indicate this fact.

‡‡ To whom correspondence should be addressed. Tel.: 61-7-3346-2033; Fax: 61-7-3346-2101; E-mail: j.hancock@mailbox.uq.edu.au.

[1] The abbreviations used are: Cav3, caveolin-3; CSD, caveolin scaffolding domain; EGF, epidermal growth factor; EGF-R, EGF receptor; AngII, angiotensin II; AT_1-R, AngII type 1 receptor; GPCR, G-protein-coupled receptor; ER, endoplasmic reticulum; HA, hemagglutinin; GFP, green fluorescent protein; BHK, baby hamster kidney; HEK, human embryonic kidney; DMEM, Dulbecco's modified Eagle's medium; FRT, Fischer rat thyroid; LDL, low density lipoprotein.

naling proteins and to sequester them in caveolae (23), although such interactions cannot be important in tethering proteins to noncaveolar lipid rafts.

The association of lipid-modified peripheral membrane proteins with lipid rafts is determined in part by the biophysical properties of the hydrophobic modification of the membrane anchor. Partitioning into rafts is favored if the lipid anchor is saturated, although in the case of prenylated and palmitoylated H-Ras activation state and additional protein sequences adjacent to the membrane anchor also influence raft association (24). Less clear is how transmembrane proteins are targeted to lipid rafts. A well studied example is the epidermal growth factor receptor (EGF-R) that is extensively localized to lipid rafts in quiescent cells (25). The receptor is not lipid-modified, but recent work has shown that a 60-amino acid region in the extracellular domain of the EGF receptor, contiguous with the transmembrane domain of the receptor, is sufficient for lipid raft targeting (26). The angiotensin II (AngII) type 1 receptor (AT_1-R) is a nonpalmitoylated G-protein-coupled receptor (GPCR) that in smooth muscle cells co-immunoprecipitates with caveolin and when activated co-fractionates with caveolin on sucrose gradients (27). The interaction between the AT_1-R and caveolin may be mediated by a CSD-binding sequence at the C terminus of the receptor (28). Similar to caveolin, the AT_1-R is found in many cell types including smooth and cardiac muscle cells as well as endothelial and epithelial cells (29). These observations have led to the hypothesis that an AT_1-R·caveolin complex in caveolae may coordinate AngII-induced signaling (27). However, in contrast to the EGF-R that exits lipid rafts following ligand binding and activation (4), activated AT_1-R moves into lipid rafts and/or caveolae where it transactivates the EGF-R (31).

Recent electron microscopic studies have shown that the EGF-R is not concentrated in caveolae (32), although similar data on the AT_1-R are lacking. In this study we used quantitative electron microscopy to examine the surface distribution of ectopically expressed AT_1-R. In addition, we show a physical interaction between the AT_1-R and caveolin and use dominant-interfering mutants of caveolin to investigate interactions between caveolin and the AT_1-R both at the plasma membrane and during trafficking through the exocytic pathway. We show that inactive AT_1-R is found in cyclodextrin-resistant and -sensitive clusters but is not enriched in surface caveolae; treatment with AngII results in the partial relocalization of activated AT_1-R into noncaveolar lipid rafts. Nevertheless, expression of mislocalized caveolin mutants, the absence of caveolin, or disrupting the formation of a caveolin·AT_1-R complex has a profound effect on the trafficking of AT_1-R from the ER to the plasma membrane. In addition, mouse studies indicate that caveolin is required for normal renal AT_1-R expression. Together these data suggest an important chaperone role for caveolin in trafficking a transmembrane receptor to the cell surface.

EXPERIMENTAL PROCEDURES

Plasmids—N-terminally HA-tagged AT_1-R (HA-AT_1-R) and C-terminally GFP-tagged AT_1-R (GFP-HA-AT_1-R) have been described (33, 34). A truncated version of the HA-AT_1-R was generated by deleting 34 amino acids C-terminal to Lys^{325} (AT_1-R,TK325) (35). AT_1-R mutants with substitutions of key hydrophobic (Tyr^{302}, Phe^{304}, Phe^{309}, and Tyr^{312}; YFFY/A) and positively charged residues (Lys^{307}, Lys^{308}, Lys^{310}, and Lys^{311}; KKKK/Q) within the proximal C terminus (helix VIII) were generated using PCR-based site-directed mutagenesis (ExSite). The template for YFFY/A was a HA-tagged version of a previously reported AT_1-R mutant (Y302A) (35), whereas the template for KKKK/Q was HA-AT_1-R. The mutant receptors were sequenced to confirm the entire coding region and the relevant nucleotide mutations. HA- and GFP-tagged full-length Cav3 (151 residues), CavDGV (residues 54–151), Cav3-P104L (Pro → Leu substitution at residue 104), HA-tagged Cav-LLS (residues 75–151), and CavDGV-G55S (residues 54–154 with a Gly → Ser substitution at residue 55) are as described (36). For GFP-tH, GFP is targeted to the plasma membrane by the minimal H-Ras anchor, which has been described previously (37). GFP-Icmt was a kind gift of Dr. Mark Philips (New York University). Caveolin-1-deficient mice have been described previously (38).

Cell Culture and Transfection—Baby hamster kidney (BHK) and Human embryonic kidney (HEK) cells were cultured at 37 °C in Dulbecco's modified Eagle's medium (DMEM) supplemented with 10% bovine calf serum. The cells were plated at 60% confluency and transfected using LipofectAMINE (Invitrogen) according to the manufacturer's instructions. After 5 h of incubation with transfection mixture, the cells were washed with serum-free medium, and medium containing 10% calf serum was added for overnight incubation. Where indicated cholesterol depletion was performed using 1% cyclodextrin (Sigma) in DMEM for 30 min following 20 h of serum starvation as described (39). Cholesterol replenishment was carried out for 1 h using a mix of 16 μg/ml cholesterol in 0.4% cyclodextrin in DMEM as described (39). Fischer rat thyroid (FRT) cells were cultured in DMEM supplemented with 10% serum supreme at 37 °C. The cells were electroporated with expression plasmids. After 24 h, the cells were processed for confocal microscopy or biochemical analysis.

Cell Fractionation—Transfected BHK cells were washed with ice-cold phosphate-buffered saline, scraped on ice into 0.3 ml of Buffer A (10 mM Tris-HCl, pH 7.5, 5 mM $MgCl_2$, 1 mM EGTA, 1 mM dithiothreitol, 1 μM $NaVO_4$, 25 mM NaF, 10 μg/ml leupeptin, and 10 μg/ml aprotinin) and homogenized through a 23-gauge needle. Post-nuclear supernatants obtained by low speed centrifugation were spun at 100,000 × *g* at 4 °C for 30 min, and the soluble fraction (S100) and the sedimented fraction (P100) were collected. The P100 fraction, which contains cellular membranes, was rinsed and resuspended in Buffer A.

Western Blotting—Protein content was measured by the Bradford reaction. 20-μg samples of the S100 and P100 fractions were separated on 10, 12, or 15% SDS-polyacrylamide gels and transferred to polyvinylidene difluoride membranes. Western blotting protein was performed using anti-HA (Babco) or anti-GFP (Roche Applied Science) antibodies. Western blots were developed using horseradish peroxidase-conjugated secondary antibodies and ECL (SuperSignal; Pierce) and quantified by phosphorimaging (Bio-Rad) as described previously (40).

Confocal Microscopy—Transfected BHK and FRT cells were washed with phosphate-buffered saline, fixed with 4% paraformaldehyde for 30 min at room temperature, and permeabilized with 0.2% Triton X-100 for 10 min. After blocking in phosphate-buffered saline containing 3% bovine serum albumin, BHK cells were incubated with anti-HA antibody in a humidified chamber for 1 h. FRT cells were incubated with an anti-Cav3 antibody (Transduction Laboratories). The cells were then washed in phosphate-buffered saline and Cy3-coupled anti-mouse secondary antisera used to visualize protein expression. The coverslips were mounted in Mowiol for confocal microscopy (37).

Electron Microscopy and Statistics—Flat sheets of plasma membrane prepared from transfected BHK cells were immunogold-labeled with anti-GFP 5-nm gold and processed for image and statistical analysis exactly as described (41, 42). Briefly, background was removed from digitized negatives using Adobe Photoshop 5.0, and the gold particle co-ordinates were determined using NIH Image 1.82. Subsequent Ripley's K-function analysis was performed using visual basic programs written into Excel macros (41, 42). Positive deflections of the *L(r)-r* curve outside the 99% confidence interval for complete spatial randomness (standardized to 1 on the figures) indicate significant clustering of the gold pattern at the radius *r* (measured in nm) at which the deviation occurs (a more detailed explanation of the statistical theory and interpretation is given in Ref. 41). The gold patterns were further evaluated using a mathematical model of plasma membrane microdomains essentially as described previously (41). Gold particles were allocated to two types of microdomain: lipid rafts with a mean radius of 20 nm or nonrafts with a mean radius of 30 nm; in addition a fraction of particles were allocated randomly over the study area. The two types of microdomain were randomly generated over the model study area and had no fixed relationship to each other. All possible relative allocations of gold particles to raft, nonraft, or the random fraction were evaluated at the gold density achieved experimentally. Twenty Monte Carlo simulations were run for each assignment of particles. The mean K-function was calculated for each model pattern, and goodness-of-fit was evaluated by calculation of the root mean square deviation from the observed data. The model giving the lowest root mean square deviation was accepted as the best fit.

Radioligand Binding—BHK cells grown in 6-well plates and HEK cells grown in 12-well plates were transfected 24 and 48 h prior to

radioreceptor assay, respectively. BHK cells were incubated in a binding buffer (50 mM Tris-HCl, 100 mM NaCl, 5 mM KCl, 5 mM $MgCl_2$, 0.6% bovine serum albumin, and 0.5 mg/ml bacitracin, pH 7.4) containing [^{125}I]Sar^1-Ile^8-AngII and appropriate levels of unlabeled AngII (0–200 ng/ml) to determine specific and nonspecific binding. After 90 min of incubation, free ligand was removed by washing three times in ice-cold binding buffer. The cells were then solubilized with 0.3 M NaOH and counted on a γ counter. HEK cell surface receptor expression was examined by the receptor binding assay described above, except the radiolabel used was [^{3}H]AngII (40 nM). Kidneys from three caveolin-1 null mice and three age-matched wild type black-6 control mice were excised, and radioreceptor assays were performed as previously described (43). AT_1-R affinity constant and expression levels were determined using Graphpad Prism (Graphpad Software Inc.). Total protein was determined by the Bradford reaction described and was used to standardize AT_1-R expression levels.

Immunoprecipitation—Transfected BHK cells were washed in ice-cold phosphate-buffered saline and scraped into 0.3 ml of Buffer B (50 mM Tris-HCl, pH 7.5, 150 mM NaCl, 4 mg/ml *n*-dodecyl β-maltoside, 0.5 mg/ml cholesteryl hemisuccinate, 1 mM phenylmethylsulfonyl fluoride, 5 μg/ml leupeptin, 1 μg/ml aprotonin, and 1 μg/ml pepstatin). After 1 h of incubation, the cells were harvested by centrifugation (14,000 $\times$ *g* for 15 min). The protein content was determined by the Bradford reaction, and 1 mg of lysate was used for immunoprecipitation. After preclearing for 2 h with agarose beads, the lysates were incubated overnight with 20 μl of protein G-agarose and mouse anti-HA antisera (1:150) or 20 μl of protein A-agarose and rabbit anti-GFP antisera (1:150). The immunoprecipitates were washed twice with ice-cold washing buffer 1 (50 mM Tris-HCl, pH 7.5, 150 mM NaCl, 1% Triton X-100, 0.5% sodium deoxycholate, 1 mM phenylmethylsulfonyl fluoride, 5 μg/ml leupeptin, 1 μg/ml aprotonin, and 1 μg/ml pepstatin), twice with washing buffer 2 (50 mM Tris-HCl, pH 7.5, 500 mM NaCl, 0.1% Triton X-100, 0.05% sodium deoxycholate), and once with washing buffer 3 (50 mM Tris-HCl, pH 7.5, 0.1% Triton X-100, 0.05% sodium deoxycholate). The proteins were eluted in 55 μl of SDS-PAGE sample buffer.

RESULTS

Activated AT_1-R Localizes to Lipid Rafts but Not Caveolae—Sucrose gradient fractionation experiments have shown that stimulation with AngII causes AT_1-R to shift from dense to light membranes that co-fractionate with caveolin (27). These data indicate that activated AT_1-R associates with lipid rafts or caveolae or both, because these microdomains have similar biophysical properties. To discriminate between these possibilities, we examined the surface distribution of AT_1-R in intact plasma membrane using electron microscopy. BHK cells expressing GFP-tagged AT_1-R were stimulated with AngII or left untreated, and apical plasma membrane sheets were ripped off directly onto electron microscopy grids. The sheets were fixed and stained with affinity-purified anti-GFP antisera coupled directly to 5-nm gold. In parallel experiments the cells were also treated with methyl β-cyclodextrin for 30 min to disrupt cholesterol-rich lipid rafts and caveolae. Caveolae are readily identifiable by their morphology, size, and labeling for caveolin. No significant labeling of caveolae for AT_1-R was evident in AngII-treated or control cells, although gold labeling was readily apparent in other areas of the plasma membrane (Fig. 1*C*). Inspection of the noncaveolar AT_1-R gold distribution suggested that it was clustered (Fig. 1*A*); we therefore analyzed the gold patterns further using spatial statistics. K-function analysis reveals that the AT_1-R is not randomly distributed over the cell surface but is localized to clusters with a mean radius of 20–30 nm (Fig. 1*D*). Cyclodextrin treatment decreased but did not cause a complete loss of clustering (Fig. 1, *B* and *D*). Stimulation with AngII for 10 min caused a significant increase in AT_1-R clustering, an effect that was blocked in the presence of cyclodextrin (Fig. 1*E*). These results indicate that unstimulated AT_1-R is resident in lipid rafts and in cholesterol-independent, nonlipid raft microdomains but that activation is accompanied by a shift of AT_1-R into cyclodextrin-sensitive lipid rafts. The extent of this movement can be estimated by mathematical modeling (Fig. 1*F*); the observed

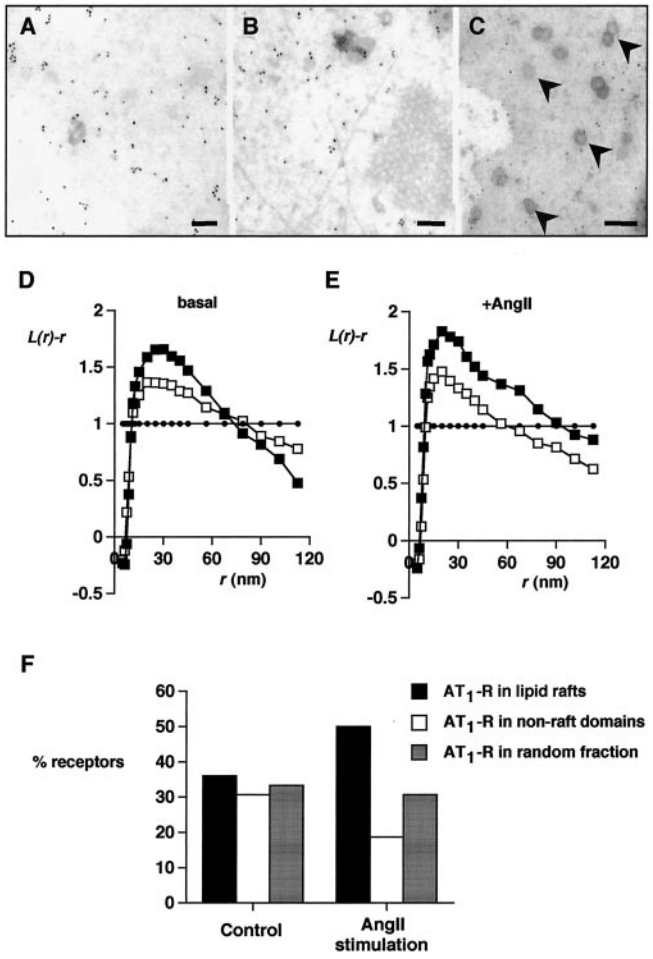

FIG. 1. **Microlocalization of GFP-AT_1-R on immunogold labeled plasma membrane sheets.** Plasma membrane sheets prepared from BHK cells expressing GFP-AT_1-R were immunogold-labeled with α-GFP-5 nm. No visual differences are apparent in the labeling for GFP-AT_1-R between basal serum-starved (*A*) and AngII-stimulated cells (*B*). Caveolae (*arrowheads*) are typically devoid of GFP-AT_1-R label (*C*). *Bars*, 100 nm; *arrowhead*, caveolae. Pooled K-function analyses of the spatial distributions of GFP-AT_1-R in basal cells (*D*) or AngII-stimulated cells (*E*) in the absence (*closed squares*) or presence (*open squares*) of 1% methyl β-cyclodextrin are shown. $L(r)$-r values above the 99% confidence interval for complete spatial randomness (*closed circles*) indicate clustering at that value of r. GFP-AT_1-R shows maximal deflections from complete spatial randomness at r = 20–30 nm for all conditions. GFP-AT_1-R clustering increases upon activation (*D* and *E*, *closed squares*). Although both inactive and stimulated GFP-AT_1-R shows some cholesterol-independent clustering, all of the increased clustering of GFP-AT_1-R induced by AngII activation is cholesterol-dependent (*i.e.* abolished by cyclodextrin treatment). K-functions are the means ($n \geq 9$ areas quantified, 500–1000 gold particles for each condition) standardized on the 99% confidence interval. *F*, a mathematical model was used to derive an estimate of the fraction of AT_1-R migrating into lipid rafts ("Experimental Procedures"). The results shown in *D* and *E* indicate that GFP-AT_1-R occupies both lipid rafts and cholesterol-independent nonraft microdomains. Multiple (385) models of AT_1-R distributed across lipid rafts and cholesterol-independent nonraft microdomains on a background of randomly distributed receptor were therefore evaluated. The relative distributions of AT_1-R that best fit the $L(r)$-r curves in *D* and *E* (*closed squares*) are shown (these models returned root mean square deviation values of 0.0529 and 0.0507, respectively).

change in AT_1-R clustering would be achieved if 40% of the AT_1-R in nonraft clusters moved into lipid rafts with AngII stimulation.

Formation of Caveolin 3·AT_1-R Complexes Is Dependent on an Intact CSD—Previous work has shown that AT_1-R co-immunoprecipitates with Cav1 from vascular smooth muscle cell lysates (27). Fig. 2 shows identical results for AT_1-R and Cav3

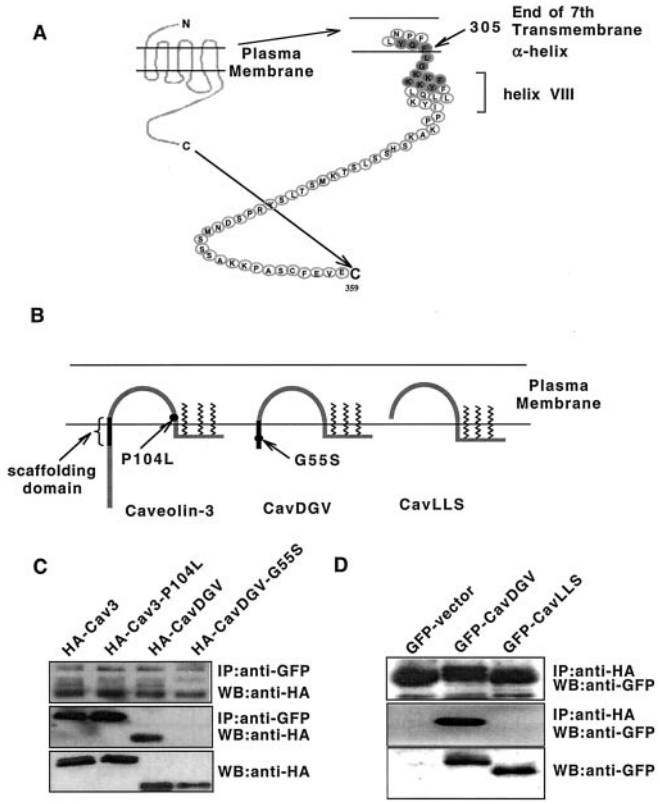

FIG. 2. **Formation of an AT_1-R·Cav3 complex requires an intact caveolin scaffolding domain.** *A*, the AT_1-R protein sequence reveals a consensus binding site (*highlighted*) for the CSD between Tyr^{302} and Tyr^{312} (^{302}Y*X*F*XXXX*F*XX*Y^{312}) comprising the C-terminal extremity of the last transmembrane domain of the receptor and the proximal C terminus (helix VIII). *B*, to determine whether the caveolin scaffolding domain (*highlighted*) is important in the formation of the Cav3·AT_1-R complex, the Cav3 mutants shown were used. *C*, BHK cells were transfected with GFP-AT_1-R (that contains both a N-terminal HA tag and a C-terminal GFP tag) alone or in combination with HA-tagged Cav3, Cav3-P104L, CavDGV, and CavDGV-G55S. An anti-GFP (polyclonal) antibody was used to immunoprecipitate (*IP*) GFP-AT_1-R. Because the receptor is also HA-tagged, AT_1-R (*top panel*) and Cav3 or Cav3 mutants (*middle panel*) are visualized by an anti-HA immunoblot. To ensure that the Cav3 constructs were expressed at detectable levels prior to immunoprecipitation, Western blot (*WB*) analysis of whole cell lysates using an anti-HA antibody was performed (*bottom panel*). *D*, BHK cells were transfected with GFP-AT_1-R in combination with empty GFP vector, GFP-CavDGV or GFP-CavLLS. AT_1-R was immunoprecipitated from cell lysates using a monoclonal anti-HA antibody. Because the AT_1-R, CavDGV, and CavLLS are all GFP-labeled, immunoblotting with a polyclonal anti-GFP antibody visualizes all of the transfected proteins present in the immunoprecipitate. Equal amounts of AT_1-R were present in all immunoprecipitates (*top panel*), whereas CavDGV but not CavLLS co-immunoprecipitated with the AT_1-R (*middle panel*). To ensure that the inability of CavLLS to immunoprecipitate with the AT_1-R was not due to a lack of CavLLS expression, Western blots of whole cell lysates were performed using an anti-GFP antibody (*bottom panel*). To determine the fraction of total Cav3 that was bound to the AT_1-R, densitometry was performed on the Cav3 immunoblots in the *middle* and *lower panels* of *C*. We estimate that ~2% of the total Cav3 in the cell lysate was complexed with the AT_1-R; this is consistent with an interaction restricted to trafficking through the exocytic pathway.

ectopically expressed in BHK cells. However, because Fig. 1 shows that the AT_1-R is not localized to surface caveolae in these cells, we investigated where else in the cell the AT_1-R·caveolin complex may form. The AT_1-R protein contains a consensus site for interaction with the CSD; the sequence, Tyr^{302}–Tyr^{312}, is located at the C-terminal extremity of the last transmembrane domain of the receptor and the proximal portion of the C terminus (Fig. 2*A*). We first examined whether an intact CSD was required to form the Cav3·AT_1-R complex using a series of previously characterized Cav3 mutants (Fig. 2*B*). CavDGV and CavLLS are N-terminal truncations at amino acids 55 and 75, respectively, such that CavDGV but not CavLLS retains the CSD. CavDGV-G55S contains a point mutation within the retained CSD. Cav3-P104L contains a naturally occurring point mutation that has been associated with mild forms of limb girdle muscular dystrophy (44). The P104L point mutation does not affect the CSD but rather prevents normal trafficking of caveolin leading to Golgi accumulation (45). Cell lysates from cells co-expressing each HA-tagged Cav3 mutant and GFP-tagged AT_1-R were normalized for AT_1-R content, immunoprecipitated with anti-GFP antiserum, and immunoblotted with anti-HA antisera. Fig. 2*C* shows that wild type Cav3, CavDGV, and Cav3-P104L all co-immunoprecipitate with the AT_1-R. However, deletion of the CSD totally abolishes the ability of CavLLS, and mutation of the CSD significantly reduces the ability of CavDGV-G55S to form stable complexes with the AT_1-R (Fig. 2, *C* and *D*). These observations show that the AT_1-R and Cav3 form a stable complex and that the CSD is critically important for Cav3/AT_1-R interaction.

Mislocalized Cav3 Mutants Sequester the AT_1-R as It Traffics to the Plasma Membrane—The preceding results suggest that the caveolin·AT_1-R complex may have a biological role other than coordinating signaling at the plasma membrane. Caveolin has recently been shown to be involved in glycosylphosphatidylinositol-linked protein trafficking to the plasma membrane (46), although no such data are available for seven transmembrane-spanning receptors. To investigate whether Cav3 was important in AT_1-R trafficking, we examined the subcellular localization of the AT_1-R in cells expressing mislocalized Cav3 mutants. In BHK cells transfected with HA-tagged AT_1-R, either alone or with wild type Cav3, the receptor was extensively localized to the plasma membrane with a small Golgi pool (Fig. 3*A*). Co-expression with CavDGV caused a striking loss of plasma membrane staining for the AT_1-R, which now localized extensively to areas containing lipid bodies marked by CavDGV. Lipid bodies are derived from the endoplasmic reticulum (11). CavLLS also accumulates in lipid bodies, but AT_1-R localized normally to the plasma membrane in CavLLS-expressing cells. Expression of Golgi-localized Cav3-P104L, however, reduced plasma membrane staining for the AT_1-R and substantially increased the Golgi pool of the receptor (Fig. 3*A*). To verify that AT_1-R mislocalization is not due to a general disruption of the exocytic pathway or ER architecture induced by the expression of mutant caveolins, we co-expressed GFP-tH (GFP appended with the minimal plasma membrane targeting sequences of H-Ras) or GFP-Icmt (isoprenyl carboxyl methyltransferase) with CavDGV and Cav3P104L (Fig. 3*B*). Neither the subcellular localization of GFP-tH, a palmitoylated, prenylated peripheral membrane protein that traffics through the exocytic pathway to the plasma membrane (37), nor GFP-Icmt, a tetraspan integral ER membrane protein (47), was affected by CavDGV or Cav3-P104L expression.

The AT_1-R undergoes endocytic recycling after activation at the plasma membrane (48). We reasoned that very little AT_1-R endocytosis was likely to occur in the absence of AngII stimulation, but to confirm that the effects of the Cav3 mutants were due to perturbations of forward traffic through the exocytic pathway, we examined the subcellular localization of an AT_1-R that is poorly internalized because of a truncation at Lys^{325} (33). The truncated receptor, AT_1-R,TK325, is expressed at a level similar to that of the wild type receptor. The AT_1-R,TK325 localized predominately to the plasma membrane of BHK cells when expressed alone or with wild type Cav3 or CavLLS. However, as with the full-length AT_1-R, co-expression with CavDGV or Cav3-P104L sequestered AT_1-TK325 to lipid bodies or the Golgi, respectively, with a concomitant loss of plasma

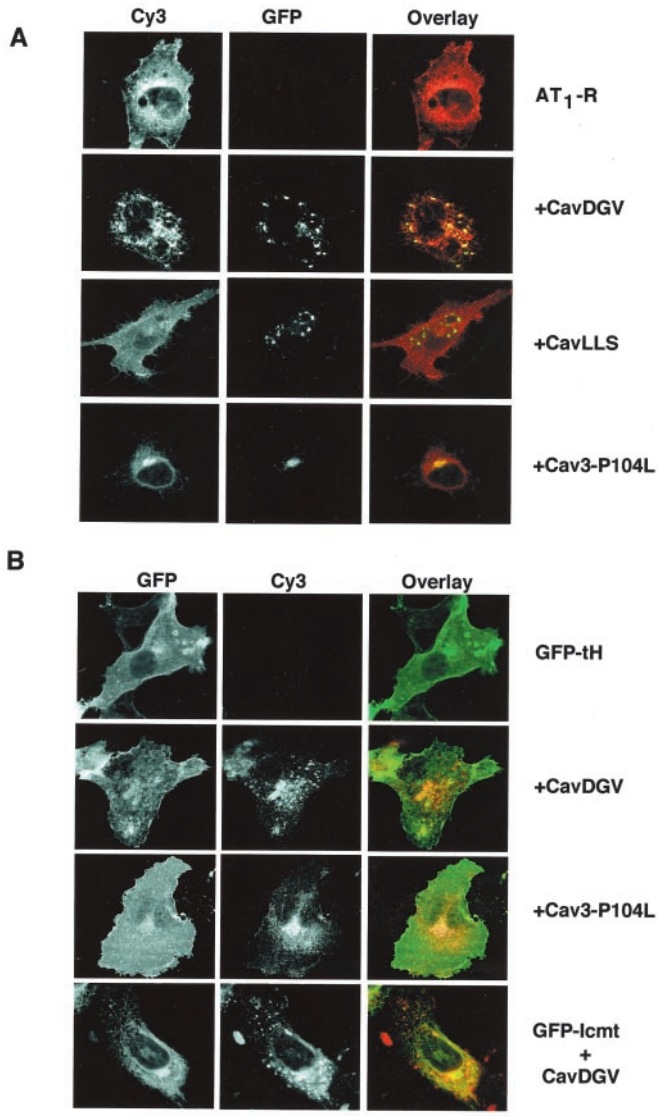

FIG. 3. **Cav3 specifically interacts with the AT_1-R in the Golgi and endoplasmic reticulum.** *A*, BHK cells were transfected with HA-tagged AT_1-R alone or in combination with mislocalized GFP-CavDGV, GFP-CavLLS, and GFP-Cav3-P104L. *B*, as controls BHK cells were transfected with GFP-tH alone or in combination with HA-tagged CavDGV and Cav3-P104L, or with GFP-Icmt and HA-tagged CavDGV (*lower panel*). GFP was visualized by direct, and HA-tagged proteins were visualized by indirect immunofluorescence. Mislocalization of Cav3 to lipid bodies (CavDGV) or the Golgi (Cav3-P104L) sequesters AT_1-R but not GFP-tH or GFP-Icmt to these structures. Although CavLLS localizes to lipid bodies, co-expression has no effect on AT_1-R localization.

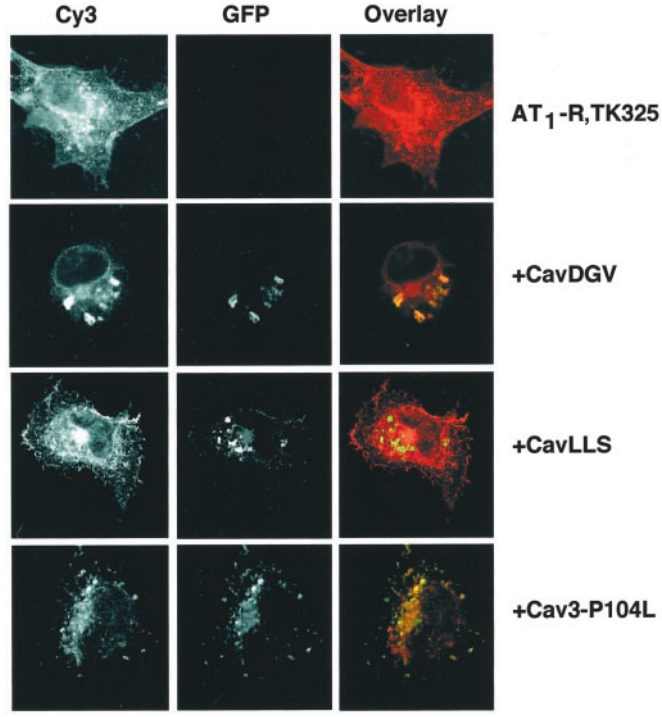

FIG. 4. **Cav3 interacts with AT_1-R in the exocytic pathway.** BHK cells were transfected with HA-tagged, truncated AT_1-R (AT_1-R,TK325) alone or in combination with mislocalized GFP-CavDGV, GFP-CavLLS, and GFP-Cav3-P104L. Mislocalization of Cav3 to lipid bodies (CavDGV) or the Golgi (Cav3-P104L) sequesters the AT_1-R,TK325 to these structures. Although CavLLS localizes to lipid bodies, co-expression has no effect on AT_1-R,TK325 localization.

membrane staining (Fig. 4). We conclude that the AT_1-R and caveolin interact at multiple stages during the exocytic pathway between the ER and the Golgi, even though there is no substantial co-localization of these proteins at the plasma membrane.

Cav3 Mutants Decrease the Expression of the AT_1-R on the Cell Surface in a Cholesterol-independent Manner—To accurately quantify the effects of impaired trafficking through the exocytic pathway, we examined changes in AT_1-R protein levels and cell surface expression by Western analysis and radioreceptor assays. Immunoblotting showed that the AT_1-R is expressed in BHK cells as a single band ~38 kDa in size representing the unglycosylated immature receptor and a smear portion ranging from 60 to 116 kDa in size representing the glycosylated or mature receptor (Fig. 5*A*). Co-expression with wild type Cav3 had no effect on AT_1-R expression or maturation (Fig. 5*A*). Co-expression of Cav3-P104L or CavDGV resulted in a significant decrease in AT_1-R expression and maturation. In contrast, CavLLS and CavDGV-G55S expression had no effect on AT_1-R expression level or maturation (Fig. 5*A*). Identical effects were seen for the noninternalizing AT_1-R,TK325 (data not shown).

To verify that changes in AT_1-R protein levels reflected cell surface expression, we performed radioreceptor assays. BHK cells transfected with the AT_1-R showed a relatively high level of receptor expression (960 ± 60 fmol/mg protein) as measured by competition binding studies using [^{125}I]Sar^1-Ile^8-AngII. These assays also revealed that the tagged receptor had a high affinity for [^{125}I]Sar^1-Ile^8-AngII (K_d = ~2.1 nM). AT_1-R ligand binding was down-regulated by co-expression of CavDGV and Cav3-P104L but was unaffected by wild type Cav3, CavDGV-G55S, or CavLLS (Fig. 5*B*). Scatchard analysis indicated that the decrease in radioligand binding was due to a decrease in receptor numbers at the cell surface and not due to a change in receptor affinity (data not shown). These results show that expression of mislocalized Cav3 mutants with an intact CSD prevent AT_1-R expression at the cell surface, consistent with a major role for caveolin in maintaining normal plasma membrane levels of the AT_1-R.

Expression of CavDGV has been shown previously to have a major effect on cholesterol distribution, resulting in a decrease in plasma membrane cholesterol and an increase in intracellular compartments (11, 49). The CavDGV-induced decrease in plasma membrane cholesterol interferes with lipid raft-dependent signaling and can be reversed by supplementing cells with exogenous cholesterol (49). We therefore investigated whether the effects of CavDGV on AT_1-R trafficking were a result of changes in cellular cholesterol. Fig. 6*A* shows that this is not the case. The reduction of AT_1-R levels in cells expressing

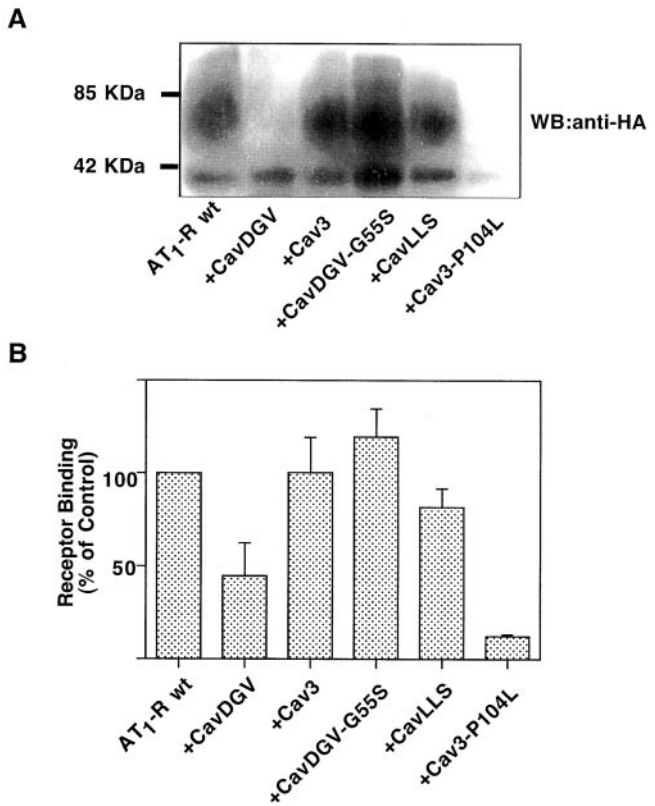

FIG. 5. **AT_1-R expression at the plasma membrane is decreased in the presence of CavDGV and Cav3-P104L.** *A*, BHK cells were transfected with HA-tagged AT_1-R alone or in combination with Cav3, CavDGV, CavLLS, CavDGV-G55S, and Cav3-P104L. P100 membrane fractions were Western blotted (*WB*) for AT_1-R using an anti-HA antibody. The AT_1-R has a lower unglycosylated (immature; molecular mass, 38–40 kDa) and a glycosylated (mature; molecular mass, 65–110 kDa) form. CavDGV and Cav3-P104L cause a significant decrease in AT_1-R expression, whereas Cav3, CavDGV-G55S, and CavLLS do not. *B*, radioreceptor assays were performed on BHK cells transfected with AT_1-R alone or in combination with Cav3 wild type or Cav3 mutants as indicated. A significant reduction of AT_1-R at the cell surface was observed in cells that co-express CavDGV or Cav3-P104L.

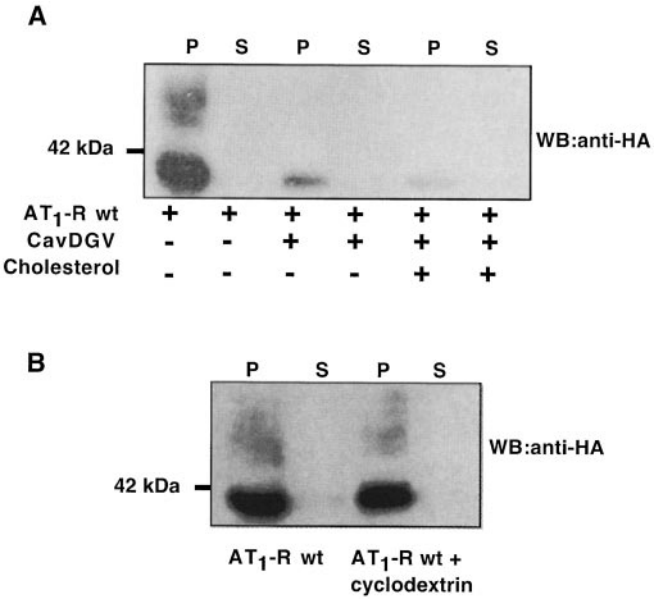

FIG. 6. **CavDGV-induced decrease in AT_1-R expression is cholesterol independent.** BHK cells transfected with AT_1-R alone or in combination with CavDGV were treated as indicated. Cell lysates were separated into P100 (P) and S100 (S) fractions, and AT_1-R was detected by Western blot using an anti-HA antibody. *A*, BHK cells co-expressing the AT_1-R and CavDGV were repleted with cholesterol for 1 h by incubation in DMEM supplemented with 16 μg/ml cholesterol in 0.4% cyclodextrin (39). *B*, BHK cells expressing the AT_1-R alone were depleted of cell surface cholesterol by incubation for 30 min in DMEM containing 1% cyclodextrin. The replenishment of cholesterol had no effect on the CavDGV-induced decrease in AT_1-R expression. Similarly cholesterol depletion had no effect on the level of AT_1-R protein expressed.

CavDGV was not alleviated by the addition of cholesterol. Furthermore mimicking the effect of CavDGV on cell surface cholesterol by treating cells with methyl β-cyclodextrin had no effect on the expression or maturation of the AT_1-R (Fig. 6*B*). We conclude that the effect of CavDGV in sequestering the AT_1-R to lipid bodies is due to the formation of a CavDGV·AT_1-R complex rather than an indirect effect on cholesterol distribution.

Mutation of the AT_1-R Putative Caveolin-binding Site Decreases AT_1-R Expression—We have shown that caveolin is important for the transport of AT_1-R to the plasma membrane and that the CSD is required for AT_1-R binding. Within the putative CSD-binding domain at the proximal end of the C-terminal tail of the AT_1-R is a group of positively charged residues that may be responsible for tethering the carboxyl tail of the AT_1-R in a conformation that allows G-protein interaction (49) and four aromatic residues that comprise the recognition sequence for CSD binding (21–23). To investigate the relative contribution of these sets of residues to AT_1-R trafficking, they were separately mutated; the four aromatic residues were replaced with alanine (AT_1-R,YFFY/A), and the charge on the four lysines was neutralized by mutation to glutamine (AT_1-R, KKKK/Q). When transfected into HEK cells, Western analysis and radioreceptor assays showed that mature AT_1-R,KKKK/Q but not AT_1-R,YFFY/A was expressed at the cell surface (Fig. 7). These results indicate that the CSD-binding site of AT_1-R but not the overlapping polybasic domain is required for trafficking to the plasma membrane. In addition, the observation that loss of the CSD-binding site affects the mature and not the immature form of the AT_1-R is consistent with the hypothesis that caveolin is required for the maturation of the receptor.

Caveolin Is Required for AT_1-R Surface Expression in FRT Cells and Mouse Kidney—All of the experiments described above were conducted in cells that express endogenous caveolin. We therefore next wanted to examine AT_1-R transport to the cell surface in cells that lack caveolin. To this end we first expressed AT_1-R in FRT cells that do not express Cav1 or Cav3 (51). Fig. 8*A* shows that AT_1-R expression in FRT cells is limited to the ER; strikingly, however, co-expression of Cav3 or Cav1 redistributes the AT_1-R from the ER to the plasma membrane. To verify the physiological significance of these observations, we investigated endogenous AT_1-R expression in Cav1 null mice using radioreceptor assays. We measured AT_1-R levels in the kidney, because they have been shown to normally co-express Cav1 (43, 52). Scatchard analysis showed that Cav1 null mice express 55% less renal AT_1-R than age-matched wild type control mice, with no change in receptor affinity (Fig. 8*B*). These data therefore indicate that wild type caveolin is required for efficient surface expression of AT_1-R in tissue culture cells and in an intact animal.

DISCUSSION

In this study we investigated the role of caveolin in AT_1-R localization and trafficking. Electron microscopy of intact plasma membrane sheets immunogold-labeled for caveolin and AT_1-R clearly shows that the receptor is not concentrated in caveolae. However, more detailed analysis of the AT_1-R immunogold patterns that decorate morphologically featureless ar-

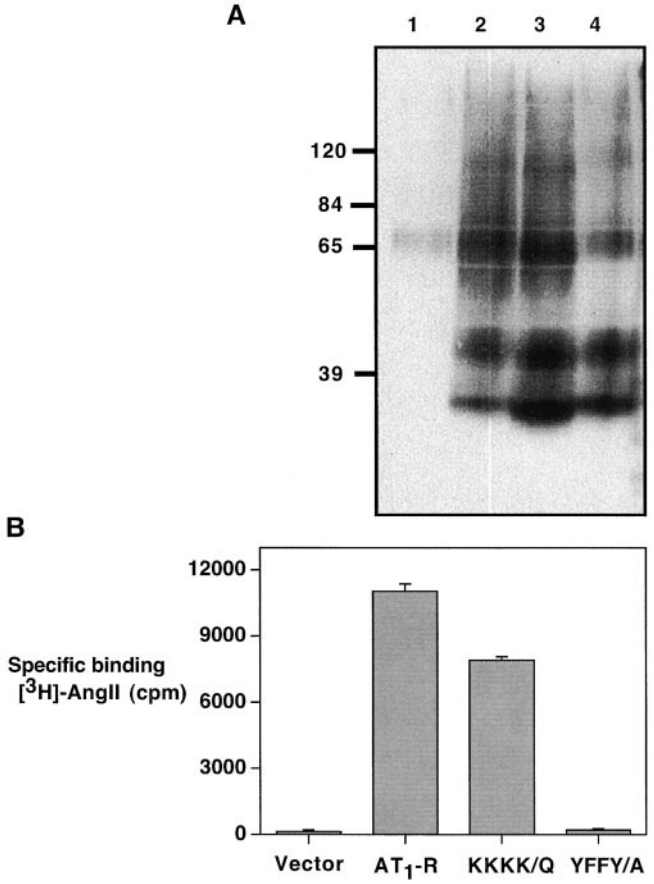

FIG. 7. **Selective mutation of the AT_1-R putative CSD binding motif reduces AT_1-R at the plasma membrane.** *A*, HEK cells were transfected with vector alone (*lane 1*), AT_1-R (*lane 2*), AT_1-R, *KKK/Q* (*lane 3*), or AT_1-R, *YFFY/A (lane 4*). Whole cell lysates were Western blotted for AT_1-R using an anti-HA antibody. In HEK cells, as in BHK cells, AT_1-R is expressed in an immature (*lower bands*) and mature (*top smear*) form. Mutation of the positively charged lysine residues (AT_1-R,KKKK/Q) in the CSD binding motif did not significantly alter the level of protein expressed. In contrast mutation of the aromatic residues (AT_1-R,YFFY/A) within the AT_1-R CSD-binding motif resulted in a dramatic decrease in the level of the mature but not the immature form of the AT_1-R. *B*, radioreceptor assays were performed on transfected HEK cells as indicated. A significant reduction of AT_1-R at the cell surface was observed in cells that expressed the AT_1-R,YFFY/A form of the AT_1-R.

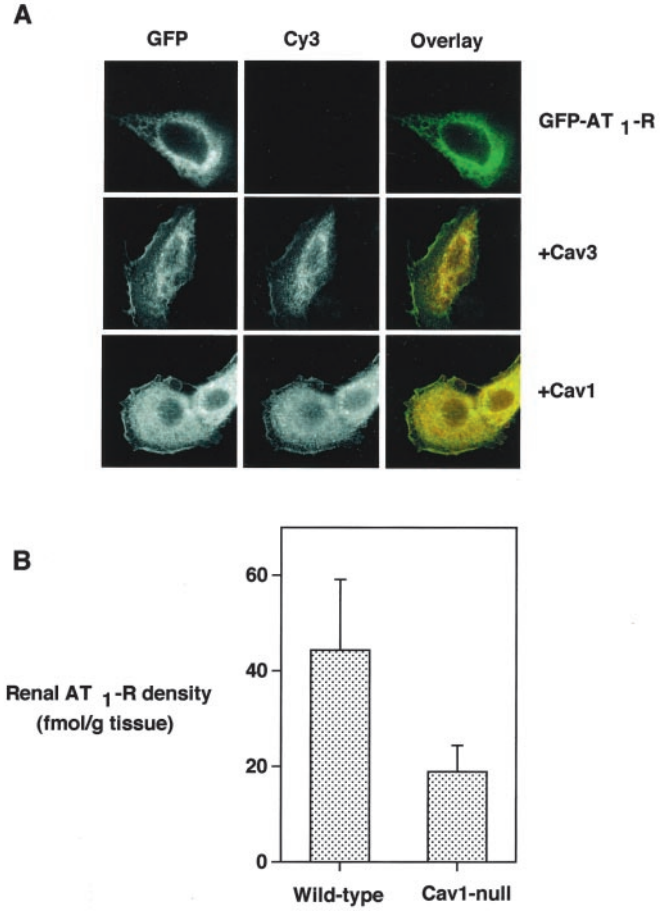

FIG. 8. **Absence of caveolin reduces AT_1-R expression *in vivo* and *in vitro*.** *A*, FRT cells were electroporated with GFP-AT_1-R alone or in combination with HA-tagged Cav3 or Cav1. GFP was visualized by direct immunofluorescence. Cav1 and Cav3 expression was detected by indirect immunofluorescence using an anti-Cav1, anti-Cav3 antibody. In the absence of ectopically expressed Cav3 or Cav1 in FRT cells (no caveolin staining), AT_1-R is exclusively expressed in the ER. Expression of Cav3 or Cav1 causes a redistribution of the AT_1-R from the ER to the plasma membrane. *B*, the kidneys of Cav1 null and wild type mice were excised, and a radioreceptor assay was performed to determine the relative level of AT_1-R expressed. Scatchard analysis indicated that wild type mice express more than twice the amount of AT_1-R than Cav1 null mice. The data shown are the means ± S.E. (n = 3). No change in receptor affinity (data not shown) between the two groups was observed.

eas of the plasma membrane reveals that the inactive AT_1-R is clustered in both cyclodextrin-resistant and cyclodextrin-sensitive microdomains. The cyclodextrin-sensitive pool is most probably AT_1-R associated with lipid rafts. The nature of the nonlipid raft microdomain is yet to be determined. Activation of the AT_1-R results in an increased degree of clustering that is completely sensitive to cyclodextrin treatment. The simplest interpretation of these results is that activation of the AT_1-R is accompanied by a migration of the receptor into lipid rafts. As with the AT_1-R, early work suggested that the EGF receptor might be localized to caveolae (25), although recent electron microscopy studies have shown that the EGF-R is actually localized to noncaveolar lipid rafts (32). The EGF-R is transactivated by the AT_1-R and mediates many AngII growth promoting effects, suggesting that the receptors must be at some stage in close proximity to each other. In light of the data presented here, we suggest that transactivation of the EGF receptor by the AT_1-R occurs in noncaveolar lipid rafts and not caveolae as previously proposed (31).

Although electron microscopy studies suggest that caveolin does not directly interact with the AT_1-R at the cell surface, several lines of evidence show that caveolin plays a central role in trafficking the AT_1-R to the plasma membrane. CavDGV sequesters the AT_1-R to lipid bodies, structures derived from the ER, leading to a decreased level of mature and immature receptor. Core glycosylation and *N*-glycosylation occur in the ER and Golgi, respectively; CavDGV must therefore bind to newly synthesized AT_1-R and prevent it traveling through the ER and Golgi. The CavDGV compartment is accessible to wild type caveolin (11), so we suggest that the AT_1-R·Cav3 complex is formed during the initial stage of AT_1-R maturation in the ER. We speculate that the AT_1-R·Cav3 complex remains intact at least until it reaches the Golgi because Golgi-localized Cav3-P104L also impairs AT_1-R forward trafficking, resulting in a significant decrease in protein and plasma membrane levels. The AT_1-R complex must then be dismantled somewhere between the Golgi and the plasma membrane or after arriving at the plasma membrane. Moreover, as expected from an interaction restricted to the exocytic pathway, only a small fraction (2%) of caveolin can be recovered from the cell lysates bound to AT_1-R. The association of the AT_1-R with lipid bodies seen by

light microscopy is itself interesting. The lipid body core is surrounded by a single phospholipid monolayer that cannot accommodate transmembrane proteins (53). We therefore envisage that the association of AT_1-R with CavDGV-induced lipid bodies might involve an enwrapping membrane system, a common feature of lipid bodies in mammalian cells (11, 53, 54). In this model, caveolin present on the cytosolic side of the lipid body would interact with the C terminus of the AT_1-R on the membrane bilayer surrounding the lipid body.

A role for caveolin in AT_1-R transport to the cell surface is also strongly supported by the observation that in FRT cells lacking Cav1 and Cav3; AT_1-R remains in the ER unless Cav1 or Cav3 are ectopically expressed. Similarly, mutation of the aromatic residues in the AT_1-R caveolin-binding motif that are known to be important for caveolin binding confines the AT_1-R to the ER and selectively reduces levels of mature but not immature receptor. Finally, we have observed that endogenous renal AT_1-R levels are substantially lower in Cav1 null mice compared with wild type controls. Caveolin has recently been identified as a trafficking chaperone for glycosylphosphatidylinositol-anchored proteins. In fibroblasts derived from Cav1 null mice, glycosylphosphatidylinositol-anchored proteins mislocalize to the Golgi, whereas ectopic expression of Cav1 or Cav3 restores plasma membrane localization (46). In the present study we have now shown that Cav1 and Cav3 also act as trafficking chaperones for a seven transmembrane-spanning GPCR. In this context, it is worth noting that Cav1 and Cav3 knockout mice suffer from a variety of cardiovascular pathologies (38, 55, 56). Given that the AT_1-R has a major role in maintaining cardiovascular homeostasis, it is tempting to speculate that alterations in AT_1-R levels, and perhaps those of other GPCRs (see below), may contribute to some of the cardiovascular changes observed in mice lacking caveolin. Interestingly Drab *et al.* (38) observed that AngII-induced vascular contractility was reduced by >50% in Cav1 null mice. In view of the results presented here, it seems likely that decreased AT_1-R levels in the vascular smooth muscle cells of Cav1 null mice contribute to this phenotype.

Does caveolin serve any other function as it traffics through the exocytic pathway in a complex with the AT_1-R? An interesting possibility is that caveolin chaperoning may prevent any interaction with other signaling proteins during maturation and transport of the AT_1-R. Some GPCR such as the β-adrenergic receptors are palmitoylated at the C terminus. Palmitic acid tethering of GPCR C-terminal to the inner leaf of the plasma membrane is important for G-protein coupling (57). A similar positioning of the nonpalmitoylated AT_1-R C terminus, however, is dependent on helix VIII and a series of charged lysine residues at positions 307–311 in this helix (50). The putative binding site for caveolin overlaps with helix VIII. Therefore, formation of the AT_1-R·Cav3 complex would certainly mask and possibly prevent correct C-terminal membrane tethering and perhaps G-protein coupling. When the caveolin·AT_1-R complex is dismantled in the Golgi or plasma membrane, the charged lysine residues would be freed, allowing formation of helix VIII and correct tethering of the C-terminal receptor tails to the plasma membrane. Interestingly, sequence analysis of other seven-transmembrane GPCRs reveals a subset that like the AT_1-R have a polylysine sequence with an overlapping putative binding sequence for the caveolin CSD immediately distal to the last transmembrane domain. These include the human somatostatin receptor type 2A, interleukin receptor type 8a, and neuropeptide Y receptor type 1. It is possible that this subset of GPCRs traffic to the plasma membrane using a mechanism similar to that of the AT_1-R.

Hypercholesterolemia is a major risk factor for cardiovascular disease. A relationship between LDL cholesterol levels and the AT_1-R has been shown by numerous studies (58–64). LDL cholesterol increases AT_1-R cell surface expression and signaling in vascular smooth muscle *in vitro* (59, 60) and *in vivo* (61). Clinical studies have also shown that hypercholesterolemic patients have an increased number of platelet AT_1-Rs and increased responsiveness to AngII infusion compared with normocholesterolemic patients (62, 63). Furthermore, HMG-CoA reductase inhibitors, which lower cholesterol, down-regulate vascular AT_1 receptors (64). These studies indicate that cholesterol regulates AT_1-R expression. Our study now shows that caveolin is necessary for correct transport of the AT_1-R to the plasma membrane. Caveolin is also up-regulated by LDL cholesterol and down-regulated by HMG-CoA reductase inhibitors (30, 65). In light of the data presented here, it is possible that the effects of cholesterol may in part reflect caveolin-mediated transport of the AT_1-R to the cell surface. Interestingly, caveolin is also involved in the post-translational regulation of endothelial nitric-oxide synthase activity. Lowering LDL cholesterol reduces caveolin levels and increases endothelial nitric-oxide synthase signaling (30). Signaling from the AT_1-R and NO are antagonistic in many of their biological functions; thus caveolin may play a role in maintaining the balance of these signaling molecules in the cardiovascular system.

Acknowledgment—We thank Mark Philips for the gift of the Icmt clone.

REFERENCES

1. Brown, D., and London, E. (1998) *Rev. Cell Dev. Biol.* **14,** 111–136
2. Kurzchalia, T. V., and Parton, R. G. (1999) *Curr. Opin. Cell Biol.* **11,** 424–431
3. Simons, K., and Ikonen, E. (1997) *Nature* **387,** 569–572
4. Mineo, C., Gill, G. N., and Anderson, R. G. W. (1999) *J. Biol. Chem.* **274,** 30636–30643
5. Prior, I. A., and Hancock, J. F. (2001) *J. Cell Sci.* **114,** 1603–1608
6. Simons, K., and Toomre, D. (2000) *Nat. Rev. Mol. Cell. Biol.* **1,** 31–39
7. Parton, R. G., Joggerst, B., and Simons, K. (1994) *J. Cell Biol.* **127,** 1199–1215
8. Anderson, R. G., Kamen, B. A., Rothberg, K. G., and Lacey, S. W. (1992) *Science* **255,** 410–411
9. Montesano, R., Roth, J., Robert, A., and Orci, L. (1982) *Nature* **296,** 651–653
10. Scheiffele, P., Verkade, P., Fra, A. M., Virta, H., Simons, K., and Ikonen, E. (1998) *J. Cell Biol.* **140,** 795–806
11. Pol, A., Luetterforst, R., Lindsay, M., Heino, S., Ikonen, E., and Parton, R. G. (2001) *J. Cell Biol.* **152,** 1057–1070
12. Rothberg, K. G., Heuser, J. E., Donzell, W. C., Ying, Y., Glenney, G. R., and Anderson, R. G. W. (1992) *Cell* **68,** 673–682
13. Scherer, P. E., Okamoto, T., Chun, M., Nishimoto, I., Lodish, H. F., and Lisanti, M. P. (1996) *Proc. Natl. Acad. Sci. U. S. A.* **93,** 131–135
14. Tang, Z-L., Scherer, P. E., Okamoto, T., Song, K., Chu, C., Kohtz, D. S., Nishimoto, I., Lodish, H. F., and Lisanti, M. P. (1996) *J. Biol. Chem.* **271,** 2255–2261
15. Murata, M., Peranen, J., Schreiner, R., Wieland, F., Kurzchalia, T. V., and Simons, K. (1995) *Proc. Natl. Acad. Sci. U. S. A.* **92,** 10339–10343
16. Schnitzer, J. E., McIntosh, D. P., Dvorak, A. M., Liu, J., and Oh, P. (1995) *Science* **269,** 1435–1439
17. Fra, A. M., Williamson, E., Simons, K., and Parton, R. G. (1995) *Proc. Natl. Acad. Sci. U. S. A.* **92,** 8655–8659
18. Zhao, Y. Y., Liu, Y., Stan, R. V., Fan, L., Gu, Y., Dalton, N., Chu, P. H., Peterson, K., Ross, J., Jr., and Chien, K. R. (2002) *Proc. Natl. Acad. Sci. U. S. A.* **99,** 11375–11380
19. Scherer, P. E., Lewis, R. Y., Volonte, D., Engelman, J. A., Galbiati, F., Couet, J., Kohtz, D. S., van Donselaar, E., Peters, P., and Lisanti, M. P. (1997) *J. Biol. Chem.* **272,** 29337–29345
20. Segal, S. S., Brett, S. E., and Sessa, W. C. (1999) *Am. J. Physiol.* **277,** H1167–H1177
21. Couet, J., Sargiacomo, M., and Lisanti, M. P. (1997) *J. Biol. Chem.* **272,** 30429–30438
22. Couet, J., Li, S., Okamoto, T., Ikezu, T., and Lisanti, M. P. (1997) *J. Biol. Chem.* **272,** 6525–6533
23. Okamoto, T., Schlegel, A., Scherer, P. E., and Lisanti, M. P. (1998) *J. Biol. Chem.* **273,** 5419–5422
24. Prior, I. A., Harding, A., Yan, J., Sluimer, J., Parton, R. G., and Hancock, J. F. (2001) *Nat. Cell Biol.* **3,** 368–375
25. Smart, E. J., Ying, Y.-S., Mineo, C., and Anderson, R. G. W. (1995) *Proc. Natl. Acad. Sci. U. S. A.* **92,** 10104–10108
26. Yamabhai, M., and Anderson, R. G. (2002) *J. Biol. Chem.* **277,** 24843–24846
27. Ishizaka, N., Griendling, K. K., Lassegue, B., and Alexander, R. W. (1998) *Hypertension* **32,** 459–466
28. Leclerc, P. C., Auger-Messier, M., Lanctot, P. M., Escher, E., Leduc, R., and Guillemette, G. (2002) *Endocrinology* **143,** 4702–4710
29. Dinh, D. T., Frauman, A. G., Johnston, C. I., and Fabiani, M. E. (2001) *Clin. Sci. (Lond.)* **100,** 481–492
30. Brouet, A., Sonveaux, P., Dessy, C., Moniotte, S., Balligand, J. L., and Feron,

O. (2001) *Circ. Res.* **89,** 866–873
31. Ushio-Fukai, M., Hilenski, L., Santanam, N., Becker, P. L., Ma, Y., Griendling, K. K., and Alexander, R. W. (2001) *J. Biol. Chem.* **276,** 48269–48275
32. Ringerike, T., Blystad, F. D., Levy, F. O., Madshus, I. H., and Stang, E. (2002) *J. Cell Sci.* **115,** 1331–1340
33. Thomas, W. G., Motel, T. J., Kule, C. E., Karoor, V., and Baker, K. M. (1998) *Mol. Endocrinol.* **12,** 1513–1524
34. Holloway, A. C., Qian, H., Pipolo, L., Ziogas, J., Miura, S., Karnik, S., Southwell, B. R., Lew, M. J., and Thomas, W. G. (2002) *Mol. Pharmacol.* **61,** 768–777
35. Thomas, W. G., Baker, K. M., Motel, T. J., and Thekkumkara, T. J. (1995) *J. Biol. Chem.* **270,** 22153–22159
36. Carozzi, A. J., Roy, S., Morrow, I. C., Pol, A., Wyse, B., Clyde-Smith, J., Prior, I. A., Nixon, S. J., Hancock, J. F., and Parton, R. G. (2002) *J. Biol. Chem.* **277,** 17944–17949
37. Apolloni, A., Prior, I. A., Lindsay, M., Parton, R. G., and Hancock, J. F. (2000) *Mol. Cell. Biol.* **20,** 2475–2487
38. Drab, M., Verkade, P., Elger, M., Kasper, M., Lohn, M., Lauterbach, B., Menne, J., Lindschau, C., Mende, F., Luft, F. C., Schedl, A., Haller, H., and Kurzchalia, T. V. (2001) *Science* **303,** 2449–2452
39. Furuchi, T., and Anderson, R. G. (1998) *J. Biol. Chem.* **273,** 21099–21104
40. Roy, S., Lane, A., Yan, J., McPherson, R., and Hancock, J. (1997) *J. Biol. Chem.* **272,** 20139–20145
41. Prior, I. A., Muncke, C., Parton, R. G., and Hancock, J. F. (2003) *J. Cell Biol.* **160,** 165–170
42. Prior, I. A., Parton, R. G., and Hancock, J. F. (2003) *Sci. STKE.* 2003, PL9
43. Wyse, B., Waters, M., and Sernia, C. (1993) *Am. J. Physiol.* **265,** E332–E339
44. Betz, R. C., Schoser, B. G., Kasper, D., Ricker, K., Ramirez, A., Stein, V., Torbergsen, T., Lee, Y. A., Nothen, M. M., Wienker, T. F., Malin, J. P., Propping, P., Reis, A., Mortier, W., Jentsch, T. J., Vorgerd, M., and Kubisch, C. (2001) *Nat. Genet.* **28,** 218–219
45. Galbiati, F., Volonte, D., Minetti, C., Chu, J. B., and Lisanti, M. P. (1999) *J. Biol. Chem.* **274,** 25632–25641
46. Sotgia, F., Razani, B., Bonuccelli, G., Schubert, W., Battista, M., Lee, H., Capozza, F., Schubert, A. L., Minetti, C., Buckley, J. T., and Lisanti, M. P. (2002) *Mol. Cell. Biol.* **22,** 3905–3926
47. Dai, Q., E. Choy, V. Chiu, J. Romano, S. R. Slivka, S. A. Seitz, S. Michaelis, S. Michaelis, and Philips, M. R. (1998) *J. Biol. Chem.* **273,** 15030–15034
48. Richard, D. E., Chretien, L., Caron, M., and Guillemette, G. (1997) *Mol. Cell. Endocrinol.* **129,** 209–218
49. Roy, S., Luetterforst, R., Harding, A., Apolloni, A., Etheridge, M., Stang, E., Rolls, B., Hancock, J. F., and Parton, R. G. (1999) *Nat. Cell Biol.* **1,** 98–105
50. Mozsolits, H., Unabia, S., Ahmad, A., Morton, C. J., Thomas, W. G., and Aguilar, M. I. (2002) *Biochemistry* **41,** 7830–7840
51. Zurzolo, C., W. van't Hof, G. van Meer, and Rodriguez-Boulan, E. (1994) *EMBO J.* **13,** 42–53
52. Zager, R. A., Johnson, A., Hanson, S., and dela Rosa, V. (2002) *Kidney Int.* **61,** 1674–1683
53. Tauchi-Sato, K., Ozeki, S., Houjou, T., Taguchi, R., and Fujimoto, T. (2002) *J. Biol. Chem.* **277,** 44507–44512
54. Prattes, S., Horl, G., Hammer, A., Blaschitz, A., Graier, W. F., Sattler, W., Zechner, R., and Steyrer, E. (2000) *J. Cell Sci.* **113,** 2977–2989
55. Woodman, S. E., Park, D. S., Cohen, A. W., Cheung, M. W., Chandra, M., Shirani, J., Tang, B., Jelicks, L. A., Kitsis, R. N., Christ, G. J., Factor, S. M., Tanowitz, H. B., and Lisanti, M. P. (2002) *J. Biol. Chem.* **277,** 38988–38997
56. Park, D. S., Woodman, S. E., Schubert, W., Cohen, A. W., Frank, P. G., Chandra, M., Shirani, J., Razani, B., Tang, B., Jelicks, L. A., Factor, S. M., Weiss, L. M., Tanowitz, H. B., and Lisanti, M. P. (2002) *Am. J. Pathol.* **160,** 2207–2217
57. Morello, J. P., and Bouvier, M. (1996) *Biochem. Cell Biol.* **74,** 449–457
58. Strehlow, K., Wassmann, S., Bohm, M., and Nickenig, G. (2000) *Ann. Med.* **32,** 386–389
59. Yang, B. C., Phillips, M. I, Mohuczy, D., Meng, H., Shen, L., Mehta, P., and Mehta, J. L. (1998) *Arterioscler. Thromb. Vasc. Biol.* **18,** 1433–1439
60. Nickenig, G., Jung, O., Strehlow, K., Zolk, O., Linz, W., Scholkens, B. A., and Bohm, M. (1997) *Am. J. Physiol.* **272,** H2701–H2707
61. Niebauer, J., Tsao, P. S., Lin, P. S., Pratt, R. E., and Cooke, J. P. (2001) *Vasc. Med.* **6,** 133–138
62. Nickenig, G., Baumer, A. T., Temur, Y., Kebben, D., Jockenhovel, F., and Bohm, M. (1999) *Circulation* **100,** 2131–2134
63. Vuagnat, A., Giacche, M., Hopkins, P. N., Azizi, M., Hunt, S. C., Vedie, B., Corvol, P., Williams, G. H., and Jeunemaitre, X. (2001) *J. Mol. Med.* **79,** 175–183
64. Ichiki, T., Takeda, K., Tokunou, T., Iino, N., Egashira, K., Shimokawa, H., Hirano, K., Kanaide, H., and Takeshita, A. (2001) *Arterioscler. Thromb. Vasc. Biol.* **21,** 1896–1901
65. Zhu, Y., Liao, H. L., Wang, N., Yuan, Y., Ma, K. S., Verna, L., and Stemerman, M. B. (2000) *Arterioscler. Thromb. Vasc. Biol.* **20,** 2465–2470